INTERNATIONAL JOURNAL OF AUTOMOTIVE AND MECHANICAL ENGINEERING
ISSN: 2229-8649 e-ISSN: 2180-1606
VOLUME 23, ISSUE 3, 2026, 13941 - 13949
DOI: https://doi.org/10.15282/ijame.23.3.2026.15.1051

RESEARCH ARTICLE

Comparison of condensation rates of surfaces mimicking the desert toktokkie beetle spot pattern and leaf vein skeleton pattern

Muhammad Hazman Saafie and Mohamad Asmidzam Ahamat*

Malaysia France Institute, Universiti Kuala Lumpur, Bandar Baru Bangi, 43650 Selangor, Malaysia

Abstract - This study investigates the condensation rate on surfaces with hydrophilic and hydrophobic patterns, inspired by the desert toktokkie beetle spot pattern and the leaf vein skeleton pattern. The objective of this study was to compare the condensation rates of surfaces inspired by the desert toktokkie beetle spot pattern and the leaf vein skeleton pattern. Five types of surfaces–the desert toktokkie beetle spot pattern, leaf vein skeleton pattern, untreated copper, PVC-coated, and laser-etched surfaces–were prepared. The measured contact angles of a water droplet on the untreated copper, PVC-coated, and laser-etched surfaces were 62.21°,101.99°, and 54.75°, respectively. Subsequently, the condensation rates of water vapour on the five surface types were measured through experiments. The heat released from condensation was measured using a thermoelectric module. The cooling power of the thermoelectric module was proportional to the condensation rate. The condensation rate of the surface with the desert toktokkie beetle spot pattern was 22.9% higher than that of the untreated copper surface. However, the condensation rate of the surface with the leaf vein skeleton pattern was only 9.53% higher than that of the untreated copper surface. The desert toktokkie beetle spot pattern induces the coalescence of droplets, which enhances the removal of condensate from the surface. The desert toktokkie beetle spot pattern also reduces the fluctuations in condensation rate by half, compared to the untreated copper surface. With appropriate adoption of features from nature, there is potential to reduce the size of a condenser.

Article History
Received : 17 July 2025
Revised : 23 September 2025
Accepted : 17 August 2026
Published : 30 September 2026

Keywords
Hydrophilic
Hydrophobic
Thermoelectric
Biomimicry
Condensation

1. Introduction

Efficient condensation is a key aim in the design of many engineering devices. For instance, efficient condensation can reduce the condenser size, enabling compact designs that require less installation space and fabrication material. Microchannels are widely adopted in refrigeration system condensers to reduce their size [1]. Microchannels significantly enhance the performance of vapour compression refrigeration systems [2]. Similar technology is also relevant to condensers in heating, ventilating, and air conditioning systems [3]. For other geometries where microchannels are not applicable, imitating nature is one approach to developing a more efficient condenser. Thus, this study compares the condensation rate of modified surfaces inspired by the desert toktokkie beetle spot pattern and the leaf vein skeleton pattern. Condensation of vapour on a surface generally occurs in two modes: dropwise or filmwise condensation. Dropwise condensation is preferred because it provides significantly higher heat transfer coefficients than filmwise condensation, as the condensate droplets are continuously removed, exposing the condenser surface to incoming vapour [4]. However, many engineering surfaces cannot sustain condensation over extended periods dropwise because the droplets eventually coalesce into a continuous liquid film [5]. Consequently, surface modification is required to promote and maintain dropwise condensation.

Surface modification involves physical or chemical alterations of the surface. The purpose of surface modification is to control the condensate behaviour during nucleation, growth, coalescence, and transport of condensate droplets, thereby enhancing the condensation heat transfer [6]. Consequently, many researchers have focused on developing surface modification techniques that promote stable dropwise condensation and improve condenser thermal performance. Combining hydrophobic and hydrophilic surfaces balances the condenser and evaporator performance [7]. This indicates that surface manipulation can be used to control the condensation rate. By varying wettability, hydrophilic, neutral, and hydrophobic serrated periodic triangular surfaces can increase the condensation rate [8]. However, these approaches involve complex surface modification, which can increase manufacturing costs. Another effort to increase the condensation rate involves the application of a vertical pattern of hydrophobic and hydrophilic surfaces [9]. However, this vertical pattern was not inspired by any features from living organisms. An ongoing debate concerns the optimal contact angle, as hydrophobic surfaces do not always enhance the condensation rate [10]. However, this hypothesis has not been investigated in the context of nature-inspired surface designs. Electrowetting promotes droplet coalescence [11]. Studies [10] - [11] have evaluated hydrophobic and hydrophilic surfaces separately, without incorporating nature-inspired design principles.

In nature, condensation rate enhancement occurs through drop jumping, sweeping, and superwetting [12] or a combination of droplet coalescence-induced jumping [13]. These methods can be mimicked to enhance the condensation rate in a condenser. In research related to bioinspired condensation surfaces, the Desert Beetle Elytra structure was fabricated using aluminium [14]. Fabricating superhydrophilic surfaces involves labourious chemical processes. This may increase the manufacturing costs of the final product. Research on micro- and dual-scale roughness has also been reported [15]. Similarly, surface fabrication involves significant technical challenges. Studies have reported the performance of

***CORRESPONDING AUTHOR | Mohamad Asmidzam Ahamat** | ✉ asmidzam@unikl.edu.my
© 2026 The Authors. Published by Universiti Malaysia Pahang Al-Sultan Abdullah Press. This is an open access article under the CC BY-NC 4.0 license

surfaces with protruded designs inspired by the Namib desert beetle, dune Bushman grass, and rice leaves for condensation in arid regions [16]. The protruded structure adopted in this study may not be necessary for condensation. Therefore, we argue that biomimetic surfaces do not require protruding surface structures to enhance the condensation rate, thereby reducing the complexity of surface modification. This study focuses on the condensation rate of biomimetic surfaces inspired by the desert toktokkie beetle (*Physasterna cribripes*) and leaf vein skeletons. The justifications for selecting the desert toktokkie beetle spot pattern and leaf vein skeleton pattern is provided here. Desert toktokkie beetles possess specialised structures on their exoskeleton that have a combination of hydrophilic and hydrophobic surfaces [17]. During the early morning, when fog blankets the desert, the beetle assumes a headstanding position, lifting its abdomen into the fog-laden breeze. As water vapour in the air contacts the beetle's body, hydrophilic surfaces promote condensation into droplets, which hydrophobic valleys then guide to its mouth once they reach a critical size [18]. For the leaf vein skeleton pattern, the shape of the vein may provide a drainage mechanism for the condensate, which could increase the rate of droplet removal, as reported in [16]. Other bio-inspired designs for collecting moisture, such as spider silk, have been reported elsewhere [19]; however, they are beyond the scope of our research. This study compares the condensation rates of modified surfaces inspired by the desert toktokkie beetle spot pattern and the leaf vein skeleton pattern. To achieve this objective, surfaces with hydrophilic and hydrophobic patterns inspired by the desert toktokkie beetle spot pattern and leaf vein skeleton pattern were fabricated. The condensation rates of water vapour on these surfaces were then measured in experiments. Finally, we discuss the condensation mechanisms on these two surfaces.

2. Materials and Methods

This section begins with the sample preparation for the condensation rate experiments and the procedure for measuring the contact angle of water droplets on their surfaces. It then describes the apparatus and procedure used to measure the condensation rate of the prepared samples and the data analysis.

2.1 Preparation of samples and contact angle measurement

2.1.1 Preparation of samples for condensation rate measurement

Five different samples with different surface conditions were prepared, as listed in Table 1. All specimens used 3 mm-thick Grade C11000 high-purity copper as their base. Each specimen had a surface area of 50 mm × 50 mm for condensation. The untreated copper surface served as the baseline for evaluating the condensation rate. A PVC-coated surface and a laser-etched surface were prepared as reference surfaces representing hydrophobic and hydrophilic conditions, respectively. The thickness of the PVC film used for coating was 0.13 mm. The desert toktokkie beetle spot pattern and the leaf vein skeleton pattern were fabricated using a two-step process: (1) laser etching at the designated positions, and (2) coating the remaining non-etched regions with a PVC film and water-repellent solution. The dimensions of the laser-etched and PVC-coated regions for the desert toktokkie beetle spot pattern and the leaf vein skeleton pattern are presented in Figures 1 and 2, respectively.

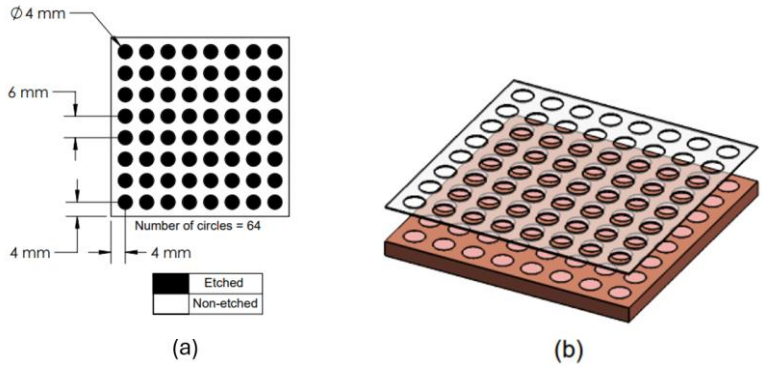


Figure 1. The geometry of the etched surface and PVC film for the desert toktokkie beetle spot pattern sample

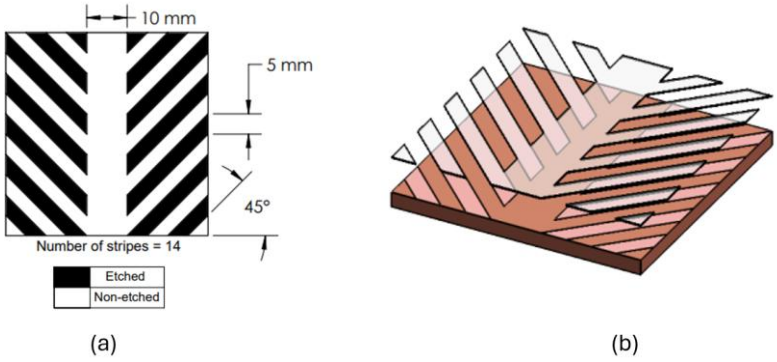


Figure 2. The geometry of the etched surface and PVC film for the leaf vein skeleton pattern sample

Table 1. Name of sample and its surface treatment

Name of sample	Type of surface modification
Untreated	No modification
PVC-coated	0.13 mm PVC film coating and water-repellent solution
Laser etched	Laser etching
Desert toktokkie beetle spot pattern Leaf vein skeleton pattern	Laser etching, 0.13 mm PVC film coating, and water-repellent solution

2.1.2 Measurement of contact angle

The untreated, laser-etched, and PVC-coated samples fabricated in Section 2.1.1 were used for contact angle measurements of a water droplet to evaluate their surface wettability. The objective of this measurement was to determine whether each surface exhibited hydrophilic or hydrophobic characteristics. Each sample was placed on a horizontal surface, and a 0.2 mL droplet of distilled water was carefully dispensed onto the surface using a syringe. A side-view image of the droplet was captured, as shown in Figure 3(a). The captured image was analysed using ImageJ software, where the droplet profile was fitted using 14 equally spaced control points (blue knots). The contact angle was subsequently determined by measuring the angle between the tangent to the fitted droplet profile at the liquid surface and the sample surface, as illustrated in Figure 3(b). The measurements were performed after the changes in contact angles became negligible (i.e., the standard deviation of the contact angle was less than 0.7°).

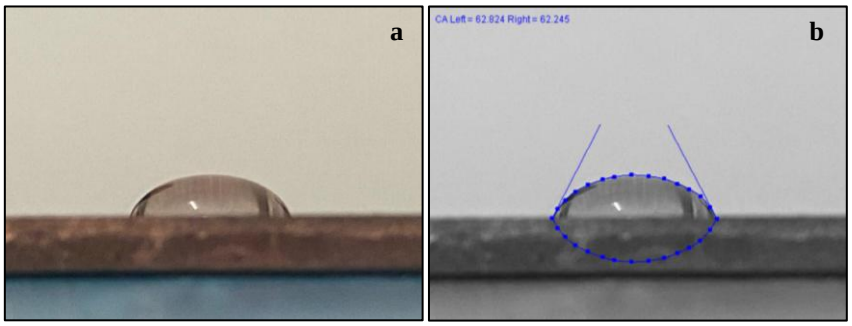


Figure 3. Measurement of the contact angle of a water droplet on an untreated copper surface: a) Formation of a water droplet on the surface, and b) contact angle measurement between the tangent to the fitted droplet profile at the liquid and the sample surface

2.2 Measurement of condensation rate

2.2.1 Apparatus

The arrangement of the experimental apparatus is shown in Figure 4. It consists of a water vapour generator, a sample, a thermoelectric module, a heat sink, a DC axial fan, an acrylic panel enclosure, and K-type thermocouples (TC_{vapour}, TC_C, and TC_H) with a PicoLog TC-08 thermocouple data logger. The water vapour generator (Model EF-501), with a rated power of 400 Watt, was used to produce steam. The steam was confined inside the acrylic panel enclosure. The influence of ambient conditions on the steam was negligible. The sample prepared in Section 2.1.1 was placed on the surface of a thermoelectric module (Model TEC1-12706) so that the heat from condensation could be dissipated from the sample. The other surface of the thermoelectric module was in contact with a heat sink and a DC axial fan. The heat sink and DC axial fan were located outside the acrylic enclosure. The dimensions of the thermoelectric module were 40 mm × 40 mm × 4 mm. The module's rated voltage and current were 12 V and 6 A, respectively. The aluminium heat sink had dimensions of 90 mm × 90 mm × 4 mm at its base. It had 14 fins with dimensions of 90 mm × 36 mm × 4 mm. The DC axial fan (Model GH9225M12S) had dimensions of 92 mm × 92 mm × 25 mm and maximum rated voltage and current of 12 V and 0.18 A, respectively. The thermocouple at position TC_{vapour} measured the temperature of the vapour near the surface of the sample. The thermocouple TC_C measured the cold surface temperature (T_C) of the thermoelectric module. The thermocouple TC_H measured the hot surface temperature (T_H) of the thermoelectric module.

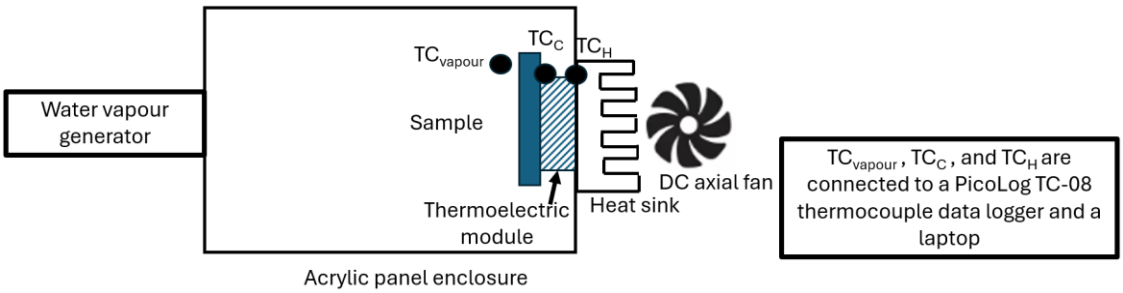


Figure 4. Schematic diagram of the experimental apparatus for condensation rate measurements

2.2.2 Experimental procedure

Throughout the experiment, the voltage supply to the thermoelectric module was maintained at 12 V, and the current was between 2.5 and 2.6 A. The DC axial fan was supplied with 12 V DC to ensure it operated at a constant speed throughout the experiment. Each experiment lasted for 50 minutes. To achieve a relatively constant heat flow through the thermoelectric module, the thermoelectric module and DC axial fan were run for 10 minutes (0^{th} to 10^{th} minute). Subsequently, the water-vapor generator was switched on to release the vapour for 30 minutes (10^{th} to 40^{th} minute). Subsequently, the experiment was continued from the 40^{th} to 50^{th} minute, with the water-vapor generator turned off. At every minute, the electrical current and temperatures were recorded. The temperature of the vapour near the surface of the sample was 85 °C ± 10 °C throughout the experiment.

2.2.3 Data and error analysis

The condensation rate was inferred from the cooling power of the thermoelectric module. The magnitude of cooling power (Q_A) on the cold surface of the thermoelectric module was calculated using Eq. 1:

$$Q_A = \alpha I T_C - \frac{1}{2} I^2 R - k(T_H - T_C) \quad (1)$$

where Q_A is the cooling power produced by the thermoelectric module (W), α is the Seebeck coefficient, taken as 0.0543 V/K, I is the electrical current; R is the electrical resistance, taken as 1.98 Ω if the average temperature of the hot and cold sides of the module is 25 °C, and 2.30 Ω for 50 °C [20]. In between, the resistance was linearly interpolated. The k is the module thermal conductivity, taken as 0.5473 W/K, T_H is the module hot surface temperature, and T_C is the module cold surface temperature. Further information for the equation is available in [21]. Throughout the experiments, the average temperature of the surfaces of the thermoelectric module is between 25 °C and 50 °C.

The sources of uncertainty that can affect the comparison of condensation rates between samples are: (1) 0.8 % due to the variation in vapour temperature (ΔQ_{vapour}), and (2) 3% due to the linear interpolation of the module's electrical resistance, and uncertainties in electrical current and temperature measurements (ΔQ_A). The total uncertainty of the cooling power($\Delta Q_{A,total}$) is estimated at 3.1%.

The derivation and equations used for the quantification of uncertainties (i.e., ΔQ_{vapour} and ΔQ_A) are available in Eq.s 2 through 5. In Eq. 2, $C_{p,vapour}$ is the specific heat of water vapour, and h_{fg} is the latent heat of water. The possible values of cooling power (i.e., maximum ($Q_{A,max}$) and minimum ($Q_{A,min}$)) were calculated using Eq. 3 and Eq. 4, respectively. Then, the greatest uncertainty was taken from the absolute difference (ΔQ_A) between $Q_{A,max}$ or $Q_{A,min}$ and Q_A, calculated using Eq. 5. Then, the total uncertainty ($\Delta Q_{A,total}$) was calculated using Eq. 6.

$$\Delta Q_{vapour} = \left(\left(C_{p,vapour} \times \Delta T_{vapour} \right) / h_{fg} \right) \times 100\% \quad (2)$$

$$Q_{A,max} = \alpha(I+\Delta I)(T_C + \Delta T_C) - \frac{1}{2}(I+\Delta I)^2 (R+\Delta R) - k((T_H + \Delta T_H) - (T_C + \Delta T_C)) \quad (3)$$

$$Q_{A,min} = \alpha(I-\Delta I)(T_C - \Delta T_C) - \frac{1}{2}(I-\Delta I)^2 (R-\Delta R) - k((T_H - \Delta T_H) - (T_C - \Delta T_C)) \quad (4)$$

$$\Delta Q_A = max(abs((Q_{A,max} - Q_A)/Q_A),\ ((Q_{A,min} - Q_A)/Q_A))\ x\,100\% \quad (5)$$

$$\Delta Q_{A,total} = \sqrt{\left(\Delta Q_{vapour}\right)^2 + (\Delta Q_A)^2} \quad (6)$$

Table 2. Uncertainty analysis

Source of uncertainty	Uncertainty, Δ	Quantification of uncertainties	Worst uncertainty
Variation in water vapour temperature			
Water vapour temperature (T_{vapour})	±10 °C	Eq. 2	0.8%
Cooling power measurement by thermoelectric module			
Electrical resistance (R)	0.0128 ohm/K	Eq. 3, Eq. 4, and Eq. 5	3%
Electrical current (I)	±0.05 Ampere		
Cold surface temperature (T_C)	± 0.5 °C		
Hot surface temperature (T_H)	± 0.5 °C		

3. Results and Discussion

This section presents the measured contact angles of water droplets on untreated, PVC-coated, and laser-etched surfaces. This section presents and discusses the condensate characteristics and condensation rates for the untreated, PVC-coated, laser-etched, desert toktokkie beetle spot, and leaf vein skeleton patterns.

3.1 Contact angle of water droplet

The purpose of contact angle measurement is to determine the hydrophobicity and hydrophilicity of the surfaces. This is essential to ensure that the modified surfaces possess the intended patterns of hydrophobicity and hydrophilicity. Thus, measurements were made for untreated, PVC-coated, and laser-etched surfaces. It is worth noting that these surfaces have no patterns to eliminate the influence of the pattern on the contact angle. The images of contact angle measurements for the untreated, PVC-coated, and laser-etched surfaces are presented in Figure 5. To reduce the measurement uncertainties, the experiment was repeated three times. The average contact angles for the untreated, PVC-coated, and laser-etched surfaces were 62.21°, 101.99°, and 54.75°, respectively. According to [6], a contact angle greater than 90° indicates a hydrophobic surface, while a contact angle less than 90° indicates a hydrophilic surface. Based on the measured contact angles, it can be concluded that the untreated and laser-etched surfaces are hydrophilic. The laser-etched treatment on the copper surface increases its level of hydrophilicity, indicated by the reduction in contact angle by 7.46°. The contact angle for the laser-etched copper surface is within the range of the value reported in [22]. The PVC-coated surface is hydrophobic, with a contact angle that is 11.99° higher than the threshold for a hydrophobic surface. The measured contact angle for the PVC-coated surface is comparable to the value reported in [23].

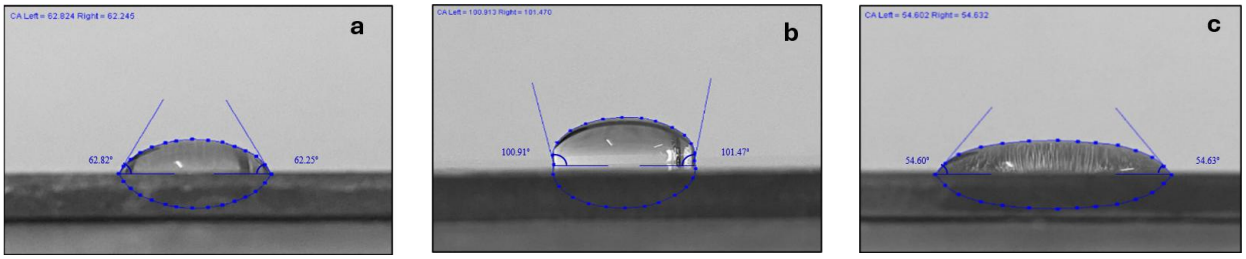


Figure 5: Contact angle measurement of a water droplet on (a) untreated, (b) PVC-coated, and (c) laser-etched surfaces

3.2 Characteristics of condensate on the surfaces

Figure 6 shows the formation of condensate on the untreated, PVC-coated, laser-etched, and desert toktokkie beetle spot pattern and leaf vein skeleton pattern surfaces. The images were taken at the end of each experiment. Generally, the sizes of the droplets on hydrophobic surfaces are larger than those on hydrophilic surfaces. In Figure 6(a), the droplets are clearly visible on the untreated surface. The sizes of the droplets on the untreated surface are larger than those on the PVC-coated surface, as shown in Figure 6(b). This indicates that the hydrophobic properties of the PVC-coated surface reduced the size of the droplets. For the laser-etched surface, as shown in Figure 6(c), the formation of water droplets was less visible than that on the untreated and PVC-coated surfaces. A thin layer of water may be trapped within the uneven profiles of the laser-etched surface.

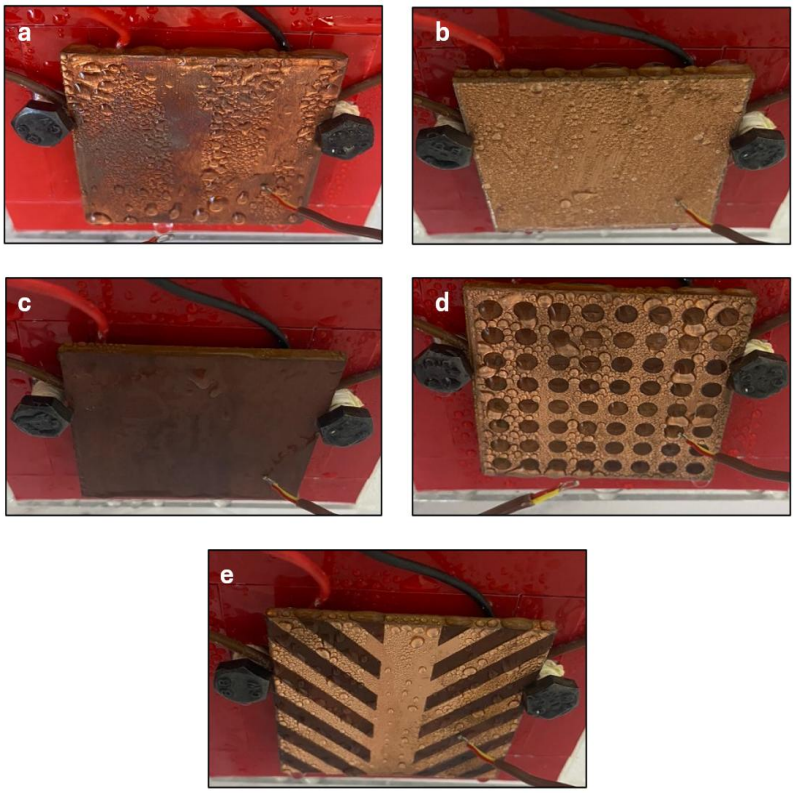


Figure 6: Condensate formation on (a) Untreated (b) PVC-coated (c) laser etched (d) desert toktokkie beetle spot pattern, and (e) leaf vein skeleton pattern samples

As shown in Figure 6(d), the density of water droplets on the desert toktokkie beetle spot pattern was higher than that on other surfaces. The characteristics of droplet formation in Figure 6(d) can be further classified into the upper (dashed box 1) and bottom (dashed box 2) regions, as shown in Figure 7(a). In dashed box 1 of Figure 7(a), larger water droplets were formed within the circular laser-etched region. The circumference of this circular laser-etched region was surrounded by smaller water droplets. In dashed box 2, more water droplets accumulated at the bottom of the surface compared to other samples. Evidence of droplet coalescence between the hydrophilic and hydrophobic regions was observed. This may increase the rate of droplet removal and make more nucleation sites available for the formation of the next droplet. Similar observations were reported in [24] for a staggered hydrophobic pattern. For the leaf vein skeleton pattern sample, as shown in Figure 6(e), there was a difference in the density of droplet formation in the hydrophilic and hydrophobic regions. A closer observation of the droplet pattern can be categorised into three regions, as detailed in Figure 7(b). The dashed box 1 has the highest density of droplet formation. Coalescence of droplets between the hydrophobic and hydrophilic surfaces was also observed. However, the size of the droplets was not significantly larger. In dashed box 2, droplet patterns similar to those of the PVC-coated temperature were observed. In dashed box 3, the density of droplets in the bottom region was less than that of the desert toktokkie beetle spot pattern sample

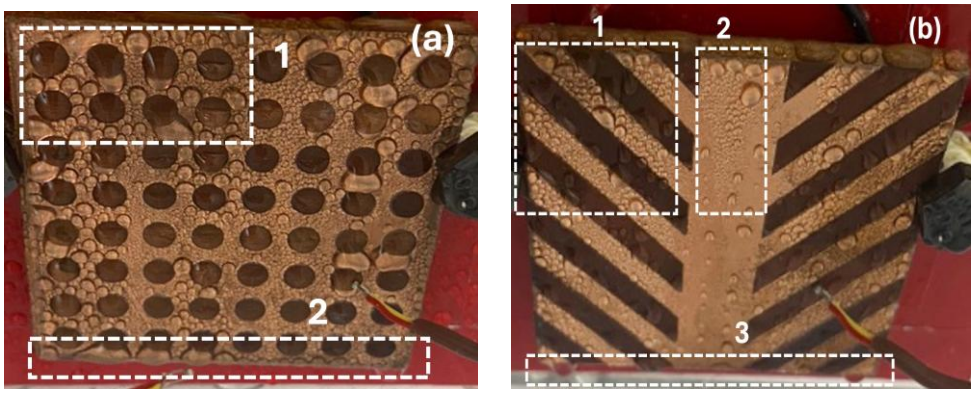


Figure 7. Condensate formation on (a) desert toktokkie beetle spot pattern, and (b) the leaf vein skeleton pattern samples

3.3 Rate of condensation

Figure 8 shows the comparison of the cooling power produced by the thermoelectric module for untreated, PVC-coated, laser-etched, desert toktokkie beetle spot pattern, and leaf vein skeleton pattern samples. The estimated uncertainty in the cooling power of the thermoelectric module was 3.1%, which made the comparison of condensation rates between the samples valid. In general, the desert toktokkie beetle spot pattern had the highest cooling power (Table 3). This can be explained by the higher density of droplets compared to other samples, as reported in Section 3.2. The desert toktokkie beetle spot pattern sample had a condensation rate that was 23% higher than the untreated surface. The untreated sample had the lowest cooling power. This means that it is necessary to modify the surface to increase its condensation rate. Another observation was on the consistency of the cooling power. The desert toktokkie beetle spot pattern sample had the lowest standard deviation in its thermoelectric cooling power, whereas the coated and etched samples had higher standard deviations. A higher standard deviation indicates inconsistency in the rate of condensation. This proves that the desert toktokkie beetle spot pattern is superior, with a relatively higher condensation rate and better consistency in the condensation rate.

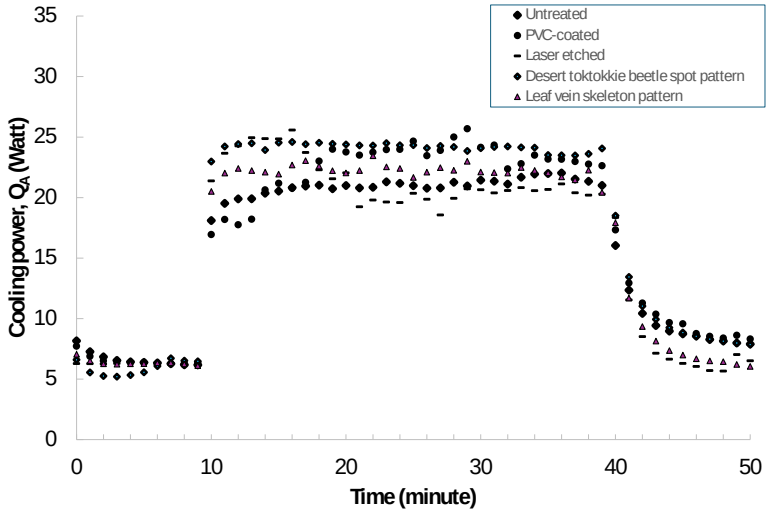


Figure 8. The cooling power of the thermoelectric module for the five samples

Table 3. The average and standard deviation of the cooling power produced by the thermoelectric module

Name of sample	Average cooling power (W)	Standard deviation of cooling power (W)	Percentage of increase compared to the untreated surface (%)
Untreated	14.61	0.58	Baseline
PVC-coated	15.88	1.96	8.73
Laser etched	15.54	1.94	6.39
Desert toktokkie beetle spot pattern	17.96	0.31	22.94
Leaf vein skeleton pattern	16.00	0.53	9.53

3.4 Discussion

The findings of this study indicate that modifying the surface to be either hydrophobic or hydrophilic alone is insufficient to significantly enhance the condensation rate. This statement is supported by the relatively small differences in condensation rates between the coated or laser-etched surfaces and the untreated surface, which were less than 9%, as shown in Table 3. In contrast, incorporating both hydrophobic and hydrophilic regions on a patterned surface improved the condensation rate, most likely by promoting more efficient condensate transport across the copper surface. However, the design of hydrophobic–hydrophilic patterns requires further optimisation. For example, the condensation rate of the leaf vein skeleton pattern surface was less than 3% higher than that of the uniformly etched or coated surfaces. Such a modest improvement may not justify the additional complexity and cost of surface modification. Therefore, the selection of an appropriate surface pattern should be carefully evaluated through technical and economic analyses. This may explain why the beetle spot pattern is frequently adopted. [25]. Otherwise, the additional cost of surface preparation may outweigh the benefits, making the overall reduction in fabrication costs difficult to justify.

The fluctuations in cooling power indicate that the condensation process is unsteady. In engineering applications, a stable condensation rate is generally preferred because it minimises fluctuations in thermal stresses within the condenser. These fluctuations may also suggest that the condensate is distributed less uniformly across the condenser surface. The fluctuations were less pronounced for the leaf vein skeleton pattern, desert toktokkie beetle spot pattern, and untreated samples. This observation suggests that the PVC-coated and laser-etched samples promote a more unsteady and potentially less uniform condensation process than the patterned surfaces. The results further indicate that incorporating hydrophobic–hydrophilic patterns on the copper surface not only enhances the condensation rate but also improves the stability and uniformity of the condensation process. A more uniform condensation process may simplify heat exchanger design by reducing localised thermal gradients and improving the predictability of condenser performance. Consequently, thermal performance models may provide more accurate predictions under steady operating conditions.

It is generally accepted that fully replicating natural surfaces is neither technically feasible nor economically feasible. For example, the surface of the desert toktokkie beetle is not flat but consists of complex and irregular hydrophobic and hydrophilic regions. Understanding this surface requires a holistic investigation under environmental conditions that closely replicate those of the natural desert habitat. Furthermore, the desert toktokkie beetle's surface properties may adapt dynamically to variations in moisture, temperature, and physiological requirements for water collection. Such adaptive characteristics involve complex interactions that are currently beyond the capabilities of existing manufacturing technologies, materials science, and control engineering disciplines. To overcome these challenges, a simplified surface design inspired by the toktokkie beetle spot pattern can be adopted. Although this design does not fully replicate the biological structure, it enables the investigation of the key mechanisms responsible for enhanced condensation while remaining practical for engineering applications and large-scale manufacturing.

The experimental method presented in this study could be further improved by increasing the cooling capacity of the thermoelectric module. A higher cooling capacity would ensure that the condensation rate is not constrained by the module, particularly when evaluating surfaces that promote enhanced condensation. In the present study, however, the thermoelectric module's cooling capacity did not appear to limit the condensation process. This is demonstrated by its ability to maintain a stable condensation rate for the desert toktokkie beetle spot pattern sample, which exhibited the lowest fluctuation in cooling power among all the tested surfaces. Another limitation of the current experimental setup is that it was designed to evaluate only flat surfaces. Because many engineering components incorporate curved or complex geometries, future studies should develop an experimental apparatus that can accurately measure condensation rates on non-flat surfaces. This improvement would broaden the method's applicability to practical engineering systems.

4. Conclusions

This study aimed to investigate the relative condensation rates on five different surfaces. Two surfaces were inspired by the desert toktokkie beetle spot pattern and the leaf vein skeleton pattern. The experimental results showed that the surface with the desert toktokkie beetle spot pattern had the highest condensation rate, which was 22.9% higher than that of the untreated surface. The condensation rate on the leaf vein skeleton pattern surface was 9.53% higher than that on the untreated surface. The condensation rate of the leaf vein skeleton pattern sample was comparable to that of the laser-etched and PVC-coated samples, which were 6–9% higher than that of the untreated sample. The condensation rate stability of the desert toktokkie beetle spot pattern sample was at least twice as good as that of the other samples. These findings show that incorporating natural design principles into engineering devices can improve condensation performance. However, a proper approach is needed because, as this study found, the leaf vein skeleton pattern sample did not show a remarkable improvement compared with the untreated copper surface sample. Because the surface

modification in this work is much less complex than in other reported research, adopting these findings in commercial engineering devices will be relatively less costly.

Acknowledgements
The authors thank Universiti Kuala Lumpur for providing the infrastructure required to conduct this research.

Funding
This study was not supported by any grants from funding bodies in the public, private, or not-for-profit sectors.

Declaration of Competing Interests
The authors declare no conflicts of interest.

CRediT Author Contribution Statement
Mohamad Asmidzam Ahamat: Conceptualisation; Supervision; Formal Analysis; Writing - Review & revise
Muhammad Hazman Saafie: Methodology; Investigation; Formal Analysis; Writing - Original Draft.

Availability of Data and Materials
Data supporting this study's findings are available upon request from the corresponding author.

Ethics Declarations
This study did not involve human participants or animal subjects. Therefore, ethical approval was not required.

Generative Artificial Intelligence Disclosure
The authors claim that artificially intelligent-assisted technologies, such as generative AI, were not used to generate content, ideas, or theories. We have utilised AI to enhance readability and refine the language. This was done with extreme human control and oversight. The authors take full responsibility for reviewing and approving the content.

References
[1] V. W. Bhatkar, V. M. Kriplani, and G. K. Awari, "Experimental analysis of microchannel condenser using R134a and drop-in substitute hydrocarbon mixture of R290 and R600a," *International Journal of Automotive and Mechanical Engineering*, vol. 10, pp. 1993–2002, 2014. https://doi.org/10.15282/ijame.10.2014.16.0167.
[2] M. Muneeshwaran, Z. Li, C. M. Yang, C. Pickles, B. Shen, and K. Nawaz, "Energy performance augmentation of domestic refrigerators with microchannel condensers," *Energy and Buildings*, vol. 359, Art. no. 117341, 2026. https://doi.org/10.1016/j.enbuild.2026.117341.
[3] N. S. Mahdi, A. A. Eidan, H. H. Abada, A. M. Sadeq, and A. E. Khatib, "Optimizing HVAC condenser design: A comprehensive review of methodologies, innovations, and efficiency enhancements," *Advances in Mechanical Engineering*, vol. 18, no. 1, 2026. https://doi.org/10.1177/16878132251408727.
[4] Y. A. Çengel and A. J. Ghajar, *Heat and Mass Transfer: Fundamentals and Applications*. New York, NY, USA: McGraw-Hill Education, 2019.
[5] B. S. Sikarwar and K. Muralidhar, "Filmwise and dropwise condensation," in *Sustainable Water Harvesting: Principles and Technologies*. Singapore: Springer Nature Singapore, 2026, pp. 81–127. https://doi.org/10.1007/978-981-95-3373-2_6.
[6] A. Goswami, S. C. Pillai, and G. McGranaghan, "Surface modifications to enhance dropwise condensation," *Surfaces and Interfaces*, vol. 25, Art. no. 101143, 2021. https://doi.org/10.1016/j.surfin.2021.101143.
[7] M. S. Irshad, G. Maqsood, N. Arshad, *et al.*, "Interfacial engineering and hydrophilic/hydrophobic coatings in solar evaporators: Strategies for balancing evaporation and condensation—A comprehensive review," *Small*, vol. 22, no. 10, Art. no. e06124, 2026. https://doi.org/10.1002/smll.202506124.
[8] Q. Liu, B. Li, L. Ma, Y. Tang, and Y. Lin, "Molecular dynamics study on water condensation on periodic triangular serrated surfaces with varying wettability," *ASME Journal of Heat and Mass Transfer*, vol. 148, no. 3, Art. no. 031603, 2026. https://doi.org/10.1115/1.4070701.
[9] S. Shahlaei, E. Aminian, M. Kamali, and H. Saffari, "Experimental study of condensation heat transfer on thermally improved hybrid Teflon-copper vertically patterned surfaces," *Heat Transfer Engineering*, vol. 47, no. 3, pp. 228–246, 2026. https://doi.org/10.1080/01457632.2024.2445914.
[10] T. K. Kulakowski, Y. Zhou, G. Celichowski, M. Psarski, and S. Adera, "Optimal contact angle for dropwise condensation: An experimental study," *International Journal of Heat and Mass Transfer*, vol. 256, Art. no. 128140, 2026. https://doi.org/10.1016/j.ijheatmasstransfer.2025.128140.
[11] S. Gao, S. Wu, L. Wu, Z. Deng, and Y. Chen, "Accelerating droplet coalescence to enhance condensation by electrowetting-on-dielectric," *International Journal of Heat and Mass Transfer*, vol. 256, Art. no. 127986, 2026. https://doi.org/10.1016/j.ijheatmasstransfer.2025.127986.
[12] R. Wang, Y. Tian, B. Shen, and X. Gao, "Bioinspired superwettability surface strategies for condensation heat transfer," *ACS Nano*, vol. 19, no. 4, pp. 4156–4169, 2025. https://doi.org/10.1021/acsnano.4c17632.

[13] M. Liu, S. Guo, L. Fang, Z. Chen, B. Xu, and X. Wang, "Dynamic characteristics of droplet coalescence-induced jumping on bioinspired symmetric rhombic microstructured surfaces," *Physics of Fluids*, vol. 37, no. 8, Art. no. 082072, 2025. https://doi.org/10.1063/5.0286483.

[14] X. Guan, Y. Peng, S. Liu, J. Ran, J. Yang, and Z. Wang, "Condensation nucleation and water collection performance of functional surfaces with hydrophilic-hydrophobic patterns inspired by desert beetle elytra," *Chemical Engineering Science*, vol. 326, Art. no. 123576, 2026. https://doi.org/10.1016/j.ces.2026.123576.

[15] C. C. Lo and L. J. Chen, "Wetting behavior-dependent heat transfer performance during dropwise condensation on engineered hydrophobic surfaces," *International Journal of Heat and Mass Transfer*, vol. 264, Art. no. 128764, 2026. https://doi.org/10.1016/j.ijheatmasstransfer.2026.128764.

[16] H. Apsey, D. Hill, and S. Alexander, "Biomimetic engineering for water harvesting: 3D printed solutions for arid regions," *RSC Applied Interfaces*, vol. 3, no. 3, pp. 776–786, 2026. https://doi.org/10.1039/d5lf00222b.

[17] A. R. Parker and C. R. Lawrence, "Water capture by a desert beetle," *Nature*, vol. 414, no. 6859, pp. 33–34, 2001. https://doi.org/10.1038/35102108.

[18] J. Guadarrama-Cetina, A. Mongruel, M. G. Medici, *et al.*, "Dew condensation on desert beetle skin," *The European Physical Journal E*, vol. 37, no. 11, Art. no. 109, 2014. https://doi.org/10.1140/epje/i2014-14109-y.

[19] H. Wei, L. Zhu, M. Zhou, *et al.*, "Bioinspired superwettable surfaces and materials for liquid motion control," *ACS Nano*, vol. 19, no. 6, pp. 5897–5912, 2025. https://doi.org/10.1021/acsnano.4c15866.

[20] HB Electronic Components, *TEC1-12706: Thermoelectric Cooler Datasheet*, Rev. 2.03. Accessed: Sep. 7, 2026. [Online]. Available: https://peltiermodules.com/peltier.datasheet/TEC1-12706.pdf

[21] M. A. Ahamat and M. J. Tierney, "Timewise temperature control with heat metering using a thermoelectric module," *Applied Thermal Engineering*, vol. 31, no. 8–9, pp. 1421–1426, 2011. https://doi.org/10.1016/j.applthermaleng.2011.01.002.

[22] M. M. Vasilev, Y. G. Shukhov, A. A. Rodionov, Y. P. Li, and M. K. Lei, "Modification of the copper wettability by nanosecond laser texturing," *Journal of Physics: Conference Series*, vol. 2119, no. 1, Art. no. 012126, 2021. https://doi.org/10.1088/1742-6596/2119/1/012126.

[23] X. Li, G. Chen, Y. Ma, *et al.*, "Preparation of a super-hydrophobic poly(vinyl chloride) surface via solvent-nonsolvent coating," *Polymer*, vol. 47, no. 2, pp. 506–509, 2006. https://doi.org/10.1016/j.polymer.2005.08.097.

[24] K. Chen, P. Gao, F. Yan, B. Cheng, D. Zhang, and X. Gao, "Analysis of condensation heat transfer on hydrophilic-hydrophobic composite surfaces considering droplets dynamic behavior," *International Journal of Heat and Mass Transfer*, vol. 247, Art. no. 127167, 2025. https://doi.org/10.1016/j.ijheatmasstransfer.2025.127167.

[25] D. Boylan, D. Monga, L. Shan, Z. Guo, and X. Dai, "Pushing the limit of beetle-inspired condensation on biphilic quasi-liquid surfaces," *Advanced Functional Materials*, vol. 33, no. 11, Art. no. 2211113, 2023. https://doi.org/10.1002/adfm.202211113.